CHEMISTRY
A EUROPEAN JOURNAL

DOI: 10.1002/chem.201103153

On the Mechanism of the Palladium-Catalyzed β-Arylation of Ester Enolates

Paolo Larini,[a] Christos E. Kefalidis,[b] Rodolphe Jazzar,[a] Alice Renaudat,[a] Eric Clot,*[b] and Olivier Baudoin*[a]

Abstract: The palladium-catalyzed β-arylation of ester enolates with aryl bromides was studied both experimentally and computationally. First, the effect of the ligand on the selectivity of the α/β-arylation reactions of *ortho*- and *meta*-fluorobromobenzene was described. Selective β-arylation was observed for the reaction of *o*-fluorobromobenzene with a range of biarylphosphine ligands, whereas α-arylation was predominantly observed with *m*-fluorobromobenzene for all ligands except DavePhos, which gave an approximate 1:1 mixture of α-/β-arylated products. Next, the effect of the substitution pattern of the aryl bromide reactant was studied with DavePhos as the ligand. We showed that electronic factors played a major role in the α/β-arylation selectivity, with electron-withdrawing substituents favoring β-arylation. Kinetic and deuterium-labeling experiments suggested that the rate-limiting step of β-arylation with DavePhos as the ligand was the palladium–enolate-to-homoenolate isomerization, which occurs by a β–H-elimination, olefin-rotation, and olefin-insertion sequence. A dimeric oxidative-addition complex, which was shown to be catalytically competent, was isolated and structurally characterized. A common mechanism for α- and β-arylation was described by DFT calculations. With DavePhos as the ligand, the pathway leading to β-arylation was kinetically favored over the pathway leading to α-arylation, with the palladium–enolate-to-homoenolate isomerization being the rate-limiting step of the β-arylation pathway and the transition state for olefin insertion its highest point. The nature of the rate-limiting step changed with PCy_3 and $PtBu_3$ ligands, and with the latter, α-arylation became kinetically favored. The trend in selectivity observed experimentally with differently substituted aryl bromides agreed well with that observed from the calculations. The presence of electron-withdrawing groups on these bromides mainly affected the α-arylation pathway by disfavoring C–C reductive elimination. The higher activity of the ligands of the biaryldialkylphosphine ligands compared to their corresponding trialkylphosphines could be attributed to stabilizing interactions between the biaryl backbone of the ligands and the metal center, thereby preventing deactivation of the β-arylation pathway.

Keywords: arylation · density functional calculations · isomerization · palladium · reaction mechanisms

Introduction

The palladium(0)-catalyzed C–H arylation α to electron-withdrawing groups such as carbonyls, nitriles, nitro groups, and sulfones has been established as a powerful method for the construction of C_{sp3}–C_{sp2} bonds.[1] Mechanistically, this reaction occurs through the oxidative addition of an aryl halide or pseudo-halide to an active palladium(0) catalyst, followed by ligand substitution to give a palladium–enolate intermediate, which provides the α-arylated product upon reductive elimination (Scheme 1, path a). Isolation of palladium-enolate intermediates and kinetic experiments have been reported to support this catalytic cycle.[2] Site-selective direct arylation of C_{sp3}–H bonds that are more remote from

[a] Dr. P. Larini,[+] Dr. R. Jazzar,[+] Dr. A. Renaudat, Prof. Dr. O. Baudoin
Université Claude Bernard Lyon 1, CNRS UMR5246
Institut de Chimie et Biochimie Moléculaires
et Supramoléculaires
CPE Lyon, 43 Boulevard du 11 Novembre 1918
69622 Villeurbanne (France)
E-mail: olivier.baudoin@univ-lyon1.fr

[b] Dr. C. E. Kefalidis,[+] Dr. E. Clot
Institut Charles Gerhardt, CNRS UMR5253
Université Montpellier 2
case courrier 1501, Place Eugène Bataillon
34095 Montpellier (France)
E-mail: clot@univ-montp2.fr

[+] These authors contributed equally to this work.

Supporting information for this article is available on the WWW under http://dx.doi.org/10.1002/chem.201103153.

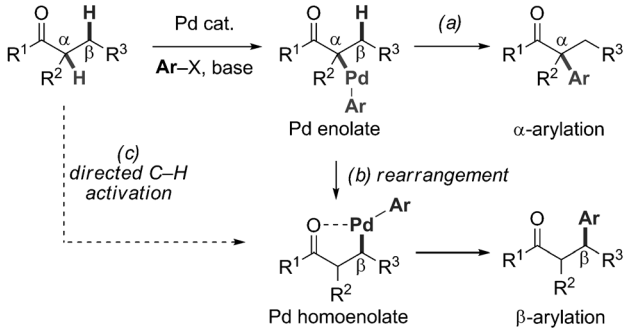

Scheme 1. Different mechanistic pathways leading to α- or β-C–H arylation.

functional groups are highly desirable given the broad synthetic utility of their corresponding products.[3] In this regard, palladium-catalyzed C–H arylations β to electron-withdrawing functional groups have been reported, most of which also employ aryl halides as convenient aryl-group donors.[4] All of these methods seem to proceed via a C–H activation mechanism (Scheme 1, path c), wherein the functional group serves as a directing group that enables the direct formation of a palladium homoenolate, which gives rise to the β-arylated product upon reductive elimination.

Building on a seminal example by Hartwig and co-workers,[5] we recently reported our preliminary results on the β-C–H arylation of carboxylic esters.[6] Our first experimental and computational data indicated that this reaction occurs through a pathway related to α-arylation (and therefore distinct to other β-arylation reactions) via the formation of an intermediate palladium enolate, rearrangement to a palladium homoenolate, and reductive elimination (Scheme 1, path b). This alternative mechanism has both advantages and drawbacks compared to the directed C–H activation mechanism. The advantages include the use of simple carboxylic esters as the reactants, which are precursors of a wide range of other functional groups, milder reaction temperature, and the fact that bis-arylation is not observed. The drawbacks include restriction of the reaction scope to enolizable esters, the need for a strong base to generate the ester enolate, and competitive α-arylation as a side-reactions. Herein, we report detailed mechanistic investigations, including both experimental and theoretical data, which shed light on this intriguing and synthetically useful C–H functionalization process and allows us to envisage new reaction extensions.

Results and Discussion

Reaction optimization and α/β-arylation selectivity: The arylation of the lithium enolate formed in situ from methyl isobutyrate (**2a**) and lithium dicyclohexylamide with 2-fluorobromobenzene (**1a**) was investigated under conditions close to those previously described by Hartwig and co-workers for an α-arylation reaction.[5] The effect of the phosphine ligand on α/β-arylation selectivity for a [Pd]/ligand ratio of 1:1 is shown in Figure 1. With P*t*Bu$_3$ as the ligand, α-arylated product **3a** was obtained in an 85:15 ratio with compound **4a**. This ratio was reversed with the less bulky tricyclohexylphosphine ligand, which afforded complete conversion and selectivity for the β-arylation product at 110 °C. However, attempts to decrease the reaction temperature failed with this ligand. Next, we turned our attention to Buchwald's biaryldicyclohexylphosphine ligands **L^1**–**L^5** (Scheme 2).[7] Apart from X-Phos (**L^3**), all of these ligands furnished complete conversion at 50 °C and high β/α selectivity. The highest selectivity was achieved with DavePhos (**L^2**), which provided the product (**4a**) with no observable trace of compound **3a**; therefore, further optimization studies were conducted with this ligand. Of the bases that were screened in

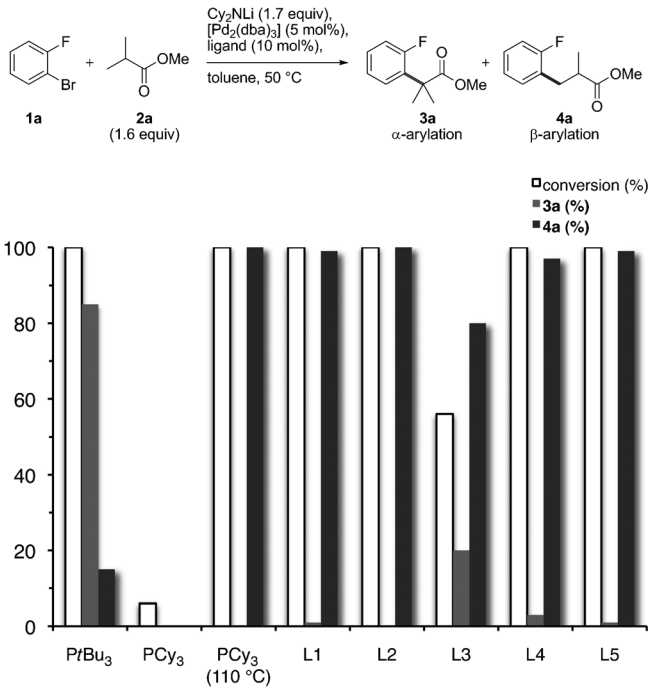

Figure 1. Effect of the ligand on the conversion and on the α/β-selectivity of the arylation of methyl isobutyrate (**2a**) with *o*-fluorobromobenzene (**1a**).

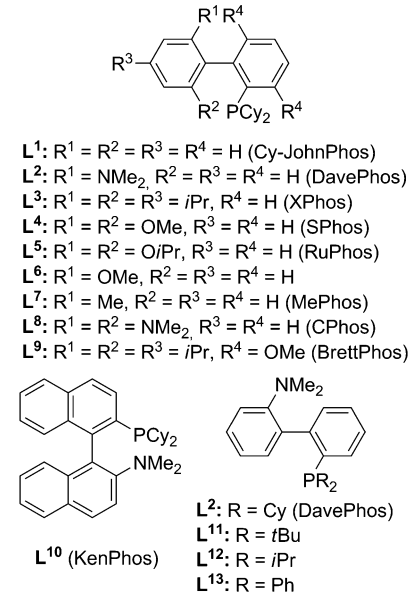

Scheme 2. Structures of biarylphosphine ligands used in this study.

combination with ester **2a**, only the strongly basic lithium amides (LDA, Cy$_2$NLi, and LiTMP) gave complete reaction conversion, which indicates that the lithium enolate of compound **2a** is indeed the reactive species. Lithium dicyclohexylamide, which tended to give higher and more-reproducible yields as reported previously,[5] was used for further studies.

Comparison of various solvents indicated that apolar, non-coordinating solvents such as toluene furnished the

highest yield of compound **4a**. Different palladium precatalysts (e.g., $[Pd_2(dba)_3]$, $Pd(OAc)_2$, and $[\{Pd(allyl)Cl\}_2]$) were evaluated in combination with different proportions of DavePhos; a 1:2 ratio of $[Pd_2(dba)_3]$ (5 mol%)/DavePhos (10 mol%) provided the highest yields with a range of substrates. A final adjustment of the ratio of enolate to aryl bromide provided the following optimal conditions, which afforded the isolated product **4a** in 69% yield: ester **2a** (1.6 equiv), Cy_2NLi (1.7 equiv), aryl bromide **1a** (1 equiv), $[Pd_2(dba)_3]$ (5 mol%), DavePhos ($\mathbf{L^2}$, 10 mol%), toluene, 30°C.[6]

Next, we studied the effect of the position of the fluorine atom with respect to the bromine atom on the aryl bromide. With the [Pd]/DavePhos catalyst, moving the fluorine substituent from the *ortho*- to the *meta*- or *para* position dramatically affected the α/β-arylation selectivity, from >99% β-arylation with an *ortho*-fluorine atom (Figure 1) to 47:53 α/β-arylation with a *meta*- or *para*-fluorine atom (Figure 2).[6] We decided to re-examine the effect of the ligand in the reaction of *m*-fluorobromobenzene (**1b**) with methyl isobutyrate (**2a**, Figure 2).

Surprisingly, from a range of commercially available or readily accessible[8] biaryldicyclohexylphosphines ($\mathbf{L^1}$–$\mathbf{L^9}$), only DavePhos ($\mathbf{L^2}$) and its methoxy analogue ($\mathbf{L^6}$)[9] provided a significant amount of β-arylated product **4b** (53% and 26%, respectively), whereas all other ligands gave complete selectivity in favor of α-arylated product **3b**. This observation stands in sharp contrast to that made with *o*-fluorobromobenzene (Figure 1), for which various biaryldicyclohexylphosphine ligands gave a high selectivity for β-arylation. By comparing unsubstituted Cy-JohnPhos ($\mathbf{L^1}$) with ligands that have a methyl ($\mathbf{L^7}$), methoxy ($\mathbf{L^6}$), or a dimethylamino ($\mathbf{L^2}$) substituent at the 2' position of the biphenyl scaffold, it appears that the more-electron-donating and/or better-coordinating NMe_2 group increases the selectivity towards β-arylation. On the other hand, if one compares mono-methoxy-substituted ligand $\mathbf{L^6}$ with bis-alkoxy-substituted ligands SPhos ($\mathbf{L^4}$) and RuPhos ($\mathbf{L^5}$), and mono-dimethylamino-substituted ligand DavePhos ($\mathbf{L^2}$) with bis-dimethylamino-substituted CPhos ($\mathbf{L^8}$),[10] it seems that the ligand flexibility at the biaryl bond also plays an important role in the α/β-arylation selectivity, with decreased flexibility giving less β-arylated product. A further indication of the importance of flexibility in the biaryl bond is shown by the trend in selectivity observed with KenPhos ($\mathbf{L^{10}}$, Scheme 2),[11] a chiral binaphthyl analogue of DavePhos for which biaryl-bond rotation is blocked. Whereas ligand $\mathbf{L^{10}}$ furnished complete β-arylation selectivity with *o*-fluorobromobenzene (**1a**), together with a promising 50% *ee*,[6] complete selectivity for the α-arylation product was again observed with *m*-fluorobromobenzene (**1b**, Figure 2). In addition, the impact of the other substituents on the phosphorus atom of DavePhos was briefly considered, with ligands $\mathbf{L^{11}}$–$\mathbf{L^{13}}$ (Scheme 2, Figure 2).[12] In the presence of the more-bulky *tert*-butyl groups instead of the cyclohexyl groups ($\mathbf{L^{11}}$),[13–14] complete selectivity for the α-arylation product was observed. On the other hand, with less-bulky isopropyl groups ($\mathbf{L^{12}}$), the selectivity for the β-arylation product decreased (56:44 ratio in favor of compound **3b**) compared to that with ligand $\mathbf{L^2}$. When the both less-bulky and electron-rich analogue $\mathbf{L^{13}}$ was used, which contained two phenyl substituents, complete selectivity for the α-arylation product was again observed. These results show that DavePhos ($\mathbf{L^2}$) possesses the optimal electronic and steric properties among the biarylphosphine ligands that were evaluated in this study of the β-arylation of methyl isobutyrate (**2a**) with *m*-fluorobromobenzene (**1b**). Finally, modifying the reaction conditions with the [Pd]/DavePhos catalytic system did not seem to affect the α/β selectivity. In particular, changing the solvent or varying the reaction temperature from 30–110°C did not modify the α/β ratio to an appreciable extent. We are currently exploring further structural modifications of DavePhos to better understand these electronic and conformational effects and to improve the β-arylation selectivity.

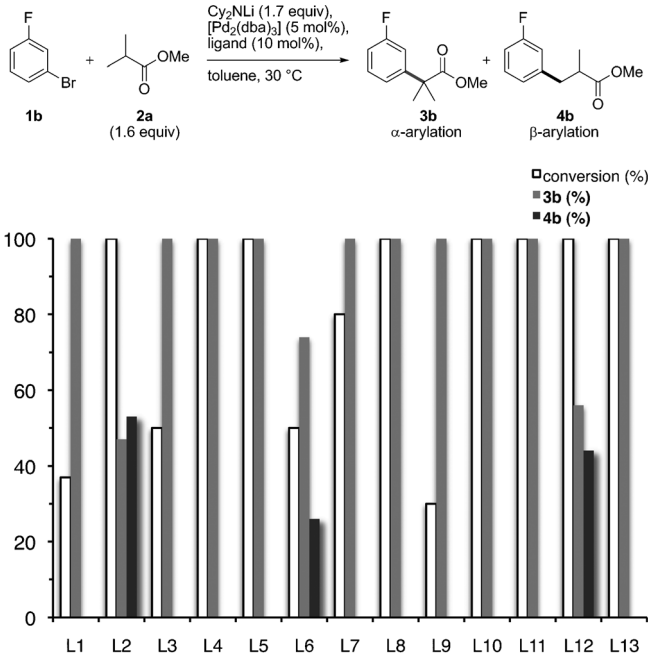

Figure 2. Effect of the ligand on the conversion and on the α/β selectivity of the arylation of methyl isobutyrate (**2a**) with *m*-fluorobromobenzene (**1b**).

With these data in hand, we studied the trend in selectivity for other aryl bromides at temperatures in the range 30–50°C (Table 1).[15] For this study, *tert*-butyl isobutyrate (**2b**) was chosen instead of methyl isobutyrate (**2a**) because the former gave cleaner reaction mixtures because of the suppression of subsequent Claisen-condensation reactions of the reaction products.[5] We confirmed that compounds **2a** and **2b** gave comparable α/β-arylation selectivities over a representative range of aryl bromides. In our first communication,[6] we showed that only *ortho*-electronegative substituents on the aryl bromide, such as F, Cl, CF_3, OCF_3, and OMe groups provided complete selectivity for β-arylation in the reaction with esters **2a** or **2b**. Table 1 shows additional examples that allow for a deeper analysis of the impact of

Table 1. Effect of the aryl-bromide structure on the β/α selectivity for the arylation of *tert*-butyl isobutyrate (**2b**).

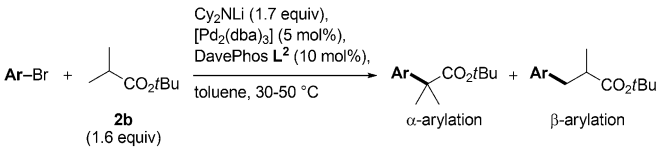

Entry	Aryl bromide	Products	α/β ratio[a]	Yield [%][b]
1	 **1a**	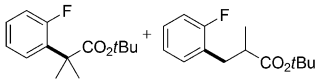 **3a'** **4a'**	<2:98	63[c]
2	 **1b**	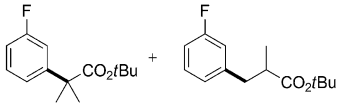 **3b'** **4b'**	47:53	95
3	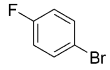 **1c**	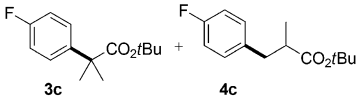 **3c** **4c**	47:53	91
4	 **1d**	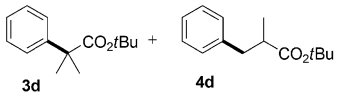 **3d** **4d**	82:18	83
5	 **1e**	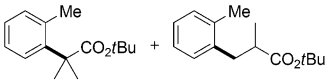 **3e** **4e**	74:26	15
6	 **1f**	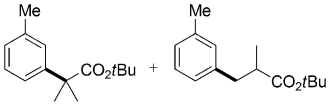 **3f** **4f**	89:11	30
7	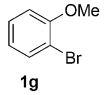 **1g**	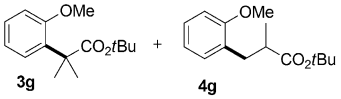 **3g** **4g**	<1:99	64[c]
8	 **1h**	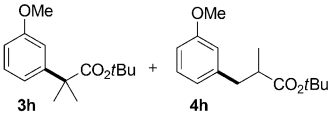 **3h** **4h**	84:16	35
9	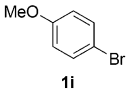 **1i**	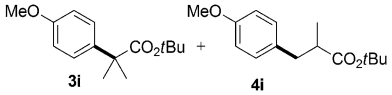 **3i** **4i**	80:20	40
10	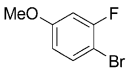 **1j**	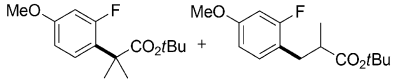 **3j** **4j**	<1:99	74[c]
11	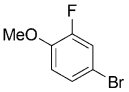 **1k**	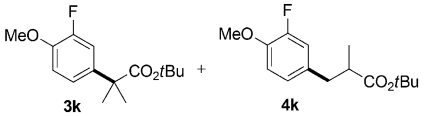 **3k** **4k**	47:53	76
12	 **1l**	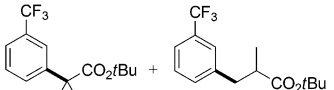 **3l** **4l**	40:60	98
13	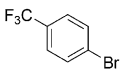 **1m**	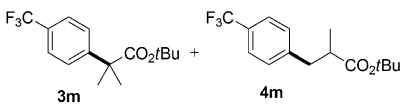 **3m** **4m**	63:37	75

the substitution pattern on the aryl-bromide on the α/β-arylation selectivity. Table 1, entries 1–3 show the effect of the position of a fluorine atom with respect to the bromine atom on the α/β-arylation selectivity (cf. Figure 1, Figure 2). With bromobenzene (**1d**), α-arylated product **3d** was the major arylation product and was obtained in an 82:18 ratio (Table 1, entry 4). As with bromobenzene, *o*-bromotoluene (**1e**) and *m*-bromotoluene (**1f**) mainly afforded their corresponding α-arylated products (**3e** and **3f**, respectively) albeit in low yields (Table 1, entries 5 and 6), which, in comparison to compounds **1a** and **1b** (Table 1, entries 1 and 2), indicates that electronic effects mainly govern the α/β-arylation selectivity with respect to the aryl bromide substrate. As shown by the comparison of Table 1, entries 5 and 6, steric effects have a minor but significant impact on the selectivity, with an *ortho* substituent favoring β-arylation. Comparison of the reactions of *ortho*-, *meta*-, and *para*-methoxybromobenzene (**1g–1i**; Table 1, entries 7–9) shows that when the methoxy group was in the *ortho* position, a high selectivity for β-arylation was observed, similar to the *ortho*-fluorine group, and almost no effect when the methoxy group was in the *meta*- and *para* positions (cf. Table 1, entry 4). The *ortho* effect of the OMe group may be ascribed to its electron-withdrawing (inductive) character at this position, whereas its electron-donating (resonance) character at the *meta*- and *para* positions does not seem to have an influence on the selectivity. The reactions of mixed fluoro/methoxy substrates **1j** and **1k** (Table 1, entries 10 and 11, respectively) showed the same trend in se-

Table 1. (Continued)

Entry	Aryl bromide	Products	α/β ratio[a]	Yield [%][b]
14	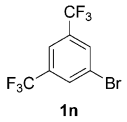 **1n**	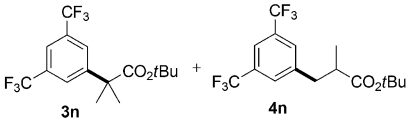 **3n** **4n**	9:91	85
15	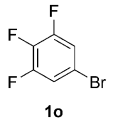 **1o**	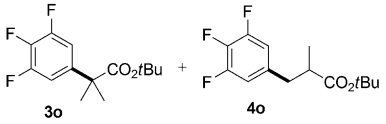 **3o** **4o**	5:95	57

[a] Measured by ^{1}H or ^{19}F NMR spectroscopy, or GCMS. [b] Measured by ^{1}H NMR spectroscopy by using trichloroethylene as an internal standard. [c] Yield of the isolated β-arylated product.

lectivity as those without a methoxy substituent (Table 1, entries 1 and 2); this result further confirms the lack of effect of the electron-donating *para*-methoxy group on the selectivity of the reaction.

Next, we examined the effect of a trifluoromethyl group at the *meta* and *para* positions was examined (Table 1, entries 12 and 13). As expected from stronger inductive effects, higher selectivity for the β-arylation product was observed with *m*-CF_3-substituted **1l**. In line with this result, and owing to the cumulative nature of inductive effects, aryl bromide **1n** , which contained two *meta*-CF_3 groups, furnished a much-higher β/α-arylation ratio (Table 1, entry 14). A similar trend was observed with 3,4,5-trifluorobromobenzene (**1o**, Table 1, entry 15), which provided a 95:5 ratio in favor of β-arylated product **4o**. These above results demonstrate that the effect of the substituents on the aryl bromide on the selectivity of the α/β-arylation reaction is mainly electronic in nature, with electron-withdrawing substituents giving more β-arylated product and no substituent or electron-donating substituents giving more α-arylated product. For a given electron-withdrawing substituent such as CF_3, this effect is maximized when the substituent is at the *ortho* position,[6] and decreases when moving this group to *meta* and *para* positions. These electronic effects are in line with DFT calculations and will be further commented on below.

Experimental mechanistic studies: We have previously proposed a common mechanism for α- and β-arylation reactions based on experimental observations and DFT calculations for the reaction of methyl isobutyrate (**2a**) and *o*-fluorobromobenzene (**1a**) using the [Pd]/PCy_3 catalytic system.[6] A modified mechanism for the same reaction catalyzed by [Pd]/DavePhos is depicted in Scheme 3.

It is well-known that the active catalyst formed with bulky biarylphosphine ligands, such as $\mathbf{L^2}$, in cross-coupling reactions is a monoligated palladium(0) complex (**Ia**), which is in equilibrium with the less-reactive [$Pd^0(L)_2$] species (**Ib**).[7,16,17] In an elementary first step, oxidative addition of aryl bromide **1a** to complex **Ia** generates complex **IIa**. Oxidative-addition complex **IIb** was prepared from a mixture of [$Pd(cod)(CH_2SiMe_3)_2$] (cod = 1,5-cyclooctadiene),[18] DavePhos ($\mathbf{L^2}$), and *o*-fluorobromobenzene (**1a**) and was characterized by single-crystal X-ray diffraction (Figure 3a).[19] X-ray structures of oxidative-addition [Pd] complexes with biarylphosphine ligands are scarce,[20] and to the best of our knowledge none has been reported with DavePhos as the ligand. Complex **IIb** shows a μ-bromo dimeric structure that features a very weak interaction between the palladium atom and the apical nitrogen atom (Pd–N distance 3.2 Å).[21]

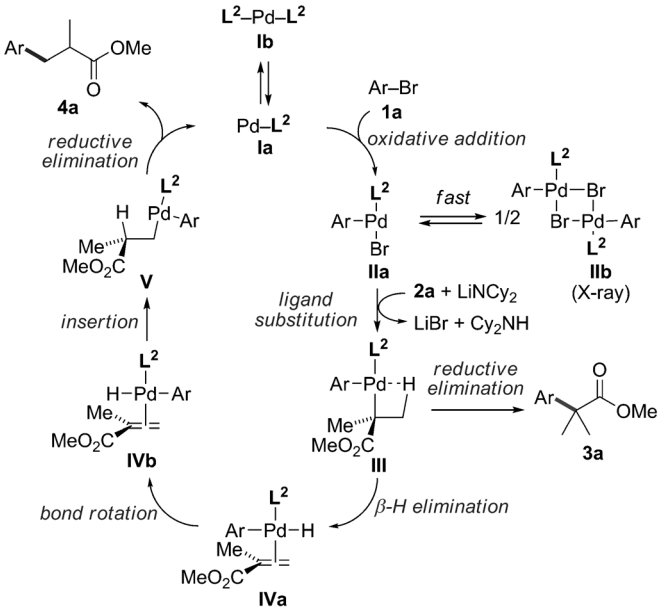

Scheme 3. Mechanism of the α- and β-arylation of methyl isobutyrate **2a** with the Pd/DavePhos catalyst (Ar = 2-fluorophenyl).

Comparison of the kinetics of the reactions of compounds **1a** and **2a**, catalyzed by **IIb** (10 mol%) or [$Pd_2(dba)_3$]/DavePhos (5 mol%/10 mol%), showed that complex **IIb** is about three times faster than the [$Pd_2(dba)_3$]/DavePhos combination; thus, complex **IIb** is a competent catalyst for this reaction (see the Supporting Information, Figure S1).[19] Dimer **IIb** is likely in fast equilibrium with monomeric species **IIa**, which lies within the catalytic cycle. A kinetic experiment involving increasing concentrations of dba showed that the dba has an inhibitory effect on the reaction (see the Supporting Information, Figure S2). This known inhibitory effect[23] may be at least partly responsible for the higher reactivity observed with isolated complex **IIb** compared to the [$Pd_2(dba)_3$]/DavePhos in situ mixture. With PCy_3 as the ligand instead of DavePhos, monometallic complex [$Pd(Ar)Br(PCy_3)_2$] (**IIc**) was isolated from the oxidative addition of compound **1a** to [$Pd(PCy_3)_2$] (Figure 3b). However, complex **IIc** was not a competent catalyst for the β-aryla-

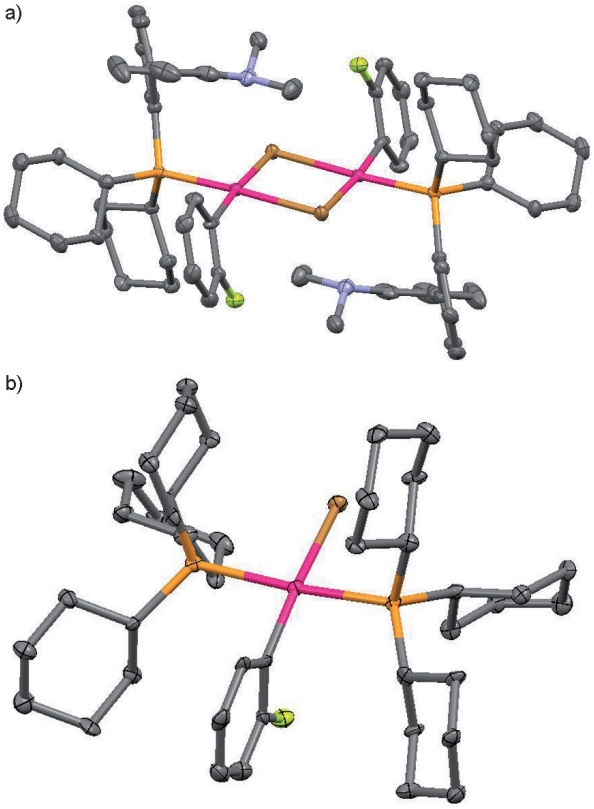

Figure 3. X-ray crystal structures of the oxidative-addition palladium-complexes a) **IIb**, obtained with compound **1a** and DavePhos, and b) **IIc**, obtained with compound **1a** and PCy_3 (thermal ellipsoids set at 30% probability, H atoms were omitted for clarity).[22]

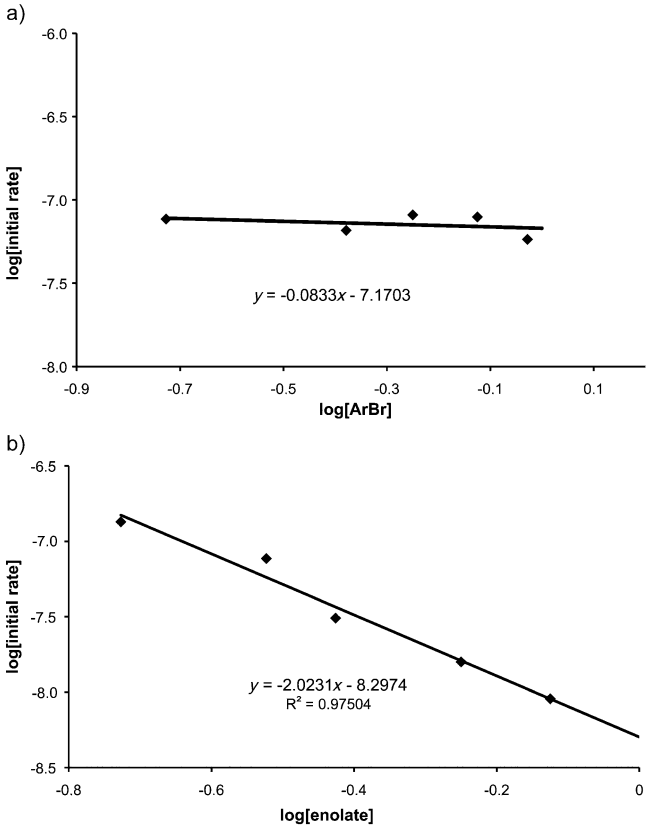

Figure 4. Logarithmic plot of the initial rate dependence on the concentration of a) *o*-fluorobromobenzene (**1a**), b) the lithium enolate of **2a** (generated in situ from a 1:1 ratio of compound **2a** and $LiNCy_2$).[19]

tion reaction of compound **2a** with compound **1a**, even at elevated temperatures, presumably because it was unable to generate the active [Pd(Ar)(Br)L] monoligated species, unlike complex **IIb**. This result may explain why the $[Pd_2(dba)_3]/PCy_3$ combination is only a competent catalyst for β-arylation at high temperatures whereas the [Pd]/DavePhos system can operate at room temperature (Figure 1).

The reaction order in *o*-fluorobromobenzene (**1a**) was determined by plotting the log of the initial rate versus the log of the concentration of compound **1a** (Figure 4a). A slope of 0.08 was obtained, thereby indicating that the reaction is zero-order in compound **1a**; therefore, oxidative addition is not rate-limiting. This observation is to be expected from the electronic properties of both the ligand (electron-rich) and the aryl bromide (electron-poor).[7]

The next step of the catalytic cycle is the substitution of the bromine atom with the lithium enolate generated in situ from ester **2a** and $LiNCy_2$ (Scheme 3). A negative order was established for the lithium enolate (Figure 4b), which shows that the reaction is inhibited by increasing the concentration of enolate and thus that the ligand-substitution step is not rate-determining either. Dicyclohexylamine is produced in stoichiometric amounts with the lithium enolate of compound **2a**; therefore, dicyclohexylamine could be also responsible for the observed reaction inhibition. An experiment with added Cy_2NH showed that the free amine indeed contributes significantly to the observed negative order in enolate, although this inhibition is less pronounced than that induced by the lithium enolate itself (see the Supporting Information, Figure S3).[19] This reaction inhibition observed with the enolate of compound **2a**, Cy_2NH, and dba might indicate that there are several catalyst-deactivation pathways. In this regard, more-precise information would be obtained by performing detailed kinetic and spectroscopic experiments; these experiments will be the subject of our future investigations. After ligand substitution (Scheme 3), palladium enolate **III** may follow two pathways: 1) reductive elimination to give α-arylated product **3a**, or 2) β–H elimination to give olefin complex **IVa**.[24] Bond rotation provides isomeric complex **IVb**, which can undergo olefin insertion either into the Pd–H or the Pd–Ar bonds. Previous calculations with PCy_3 as the ligand indicated that the former insertion is much-more-kinetically favored than the latter.[6] The corresponding palladium homoenolate **V** then undergoes reductive elimination to give β-arylated product **4a** and initial complex **Ia**.

To gain an insight into the steps following ligand substitution (i.e., isomerization of palladium enolate **III** into homoenolate **V** and reductive elimination; Scheme 3), the reactivity of deuterium-labeled esters **2c–2e** was analyzed (Scheme 4).[25] The reaction of ester **2c**, which had a deuteri-

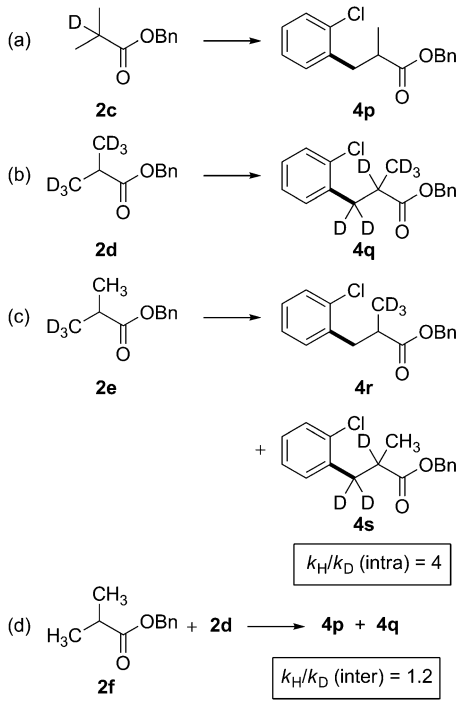

Scheme 4. β-Arylation experiments with deuterated esters. Reaction conditions: ester (1.6 equiv), Cy_2NLi (1.7 equiv), 2-chlorobromobenzene (**1p**, 1.0 equiv), $[Pd_2(dba)_3]$ (5 mol%), DavePhos (**L²**, 10 mol%), toluene, 25°C. Kinetic isotope effects were measured by ^1H NMR spectroscopy. Cy = cyclohexyl, dba = dibenzylideneacetone.

um atom at the α-position, gave product **4p**, which showed no trace of deuterium (Scheme 4a). From starting ester **2d**, which had fully deuterated β-positions and a protonated α-position, product **4q** showed a complete D shift onto the α-position (Scheme 4b). These two experiments are consistent with the proposed mechanism (Scheme 3) and rule out a directed-C–H-activation mechanism (Scheme 1, path c). An intramolecular kinetic isotope effect (KIE) was then determined from the reaction of ester **2e**, which provided a k_H/k_D value of 4.0 (Scheme 4c).[26] The corresponding intermolecular KIE value was measured by reacting a 1:1 ratio of esters **2f** and **2d** and analyzing the ratio of products **4p** and **4q** at various conversions (Scheme 4d). A constant **4p**/**4q** ratio of 1.2 was obtained, which corresponded to a k_H/k_D value of 1.2. The important difference between the intra- and intermolecular isotope effects indicates that the β–H-elimination (**III**→**IVa**) or olefin-insertion steps (**IVb**→**V**) alone are not rate-determining. However, the significant intermolecular effect ($k_H/k_D > 1$) implies that either the β–H-elimination or the olefin-insertion steps has a significant impact on the reaction rate.

Overall, the kinetic experiments indicate that the first elementary steps of the catalytic cycle (Scheme 3), that is oxidative addition and ligand substitution, are not rate-determining. The impact of the subsequent steps on the reaction kinetics, as assessed by deuterium-labeling experiments, seems ambiguous at the moment. The magnitude of the intra- and intermolecular isotope effects suggests that the overall isomerization of palladium enolate **III** into palladium homoenolate **V**, involving the β–H-elimination/olefin-rotation/olefin-insertion sequence,[27] is rate-determining.[28] At this stage, DFT calculations were deemed necessary to complete this mechanistic picture. In particular, these calculations were expected to provide more insight into the relative influence of the different elementary steps on the reaction rate and on the selectivity for α-/β-arylation.

Computational studies: The mechanism of the reaction of compound **1a** with compound **2a**, catalyzed by [Pd(DavePhos)], was studied computationally at the B3PW91 level.[29] The actual biarylphosphine ligand DavePhos was considered in the calculations. The extrema were located in the gas phase and the energies given below are polarizable continuum model (PCM) electronic energy values (toluene) corrected by gas phase Gibbs free energy contributions.[19] As the C–Br oxidative-addition and ligand-substitution steps were shown experimentally not to be rate-determining, the computational study concentrated on the sequence of steps from enolate complex **III** to the regeneration of active catalyst **Ia** (Scheme 3). Given the asymmetry of the DavePhos ligand and of the *ortho*-fluoro-substituted aryl group of compound **1a**, there are in principle eight different possible geometries for enolate **III**. For the optimization of six of these possibilities, we assumed that the situation where the ester OMe group points toward the biaryl moiety was disfavored on steric grounds (see the Supporting Information, Figure S4).[19] In most cases, the energetically preferred geometries were where the *ortho*-fluoro group was on the same side of the molecule as the biaryl group of DavePhos. In addition, the ester OMe group preferred a position that avoided the biaryl group on the phosphine ligand (**IIIa**; Figure 5). The mechanisms of the α- and β-arylation reactions were computed for the most-stable isomer (**IIIa**). The geometry of isomer **IIIa** is pseudo-square-planar with the enolate

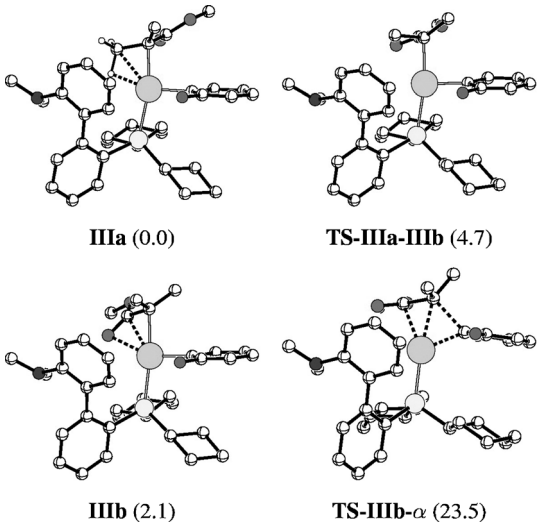

Figure 5. Optimized geometry and Gibbs free energy (kcal mol^{-1}, relative to complex **IIIa**) of the various intermediates and transitions states along the α-arylation pathway.

group bonded through the α-carbon atom *trans* to the phosphorous atom (Pd–C_α 2.082 Å, Pd–Ar 2.016 Å); a β–CH agostic interaction (C_β–H 1.160 Å, H···Pd 1.909 Å) completes the coordination sphere around the Pd^{II} center. The pathway for α-arylation starts with an isomerization from compound **IIIa** into isomer **IIIb**, which is an intermediate that features a Pd···O interaction *trans* to the aryl group (2.281 Å). This intermediate is 2.1 kcal mol^{-1} higher in energy than isomer **IIIa**; the transition state (TS; **TS-IIIa-IIIb**) is associated to rotation of the enolate ligand around the Pd–C_α bond and is 4.7 kcal mol^{-1} higher in energy than isomer **IIIa**. From isomer **IIIb**, the C–C reductive coupling that leads to α-arylated product **3a** proceeds through **TS-IIIb-α** with a Gibbs free energy that is 23.5 kcal mol^{-1} higher than isomer **IIIa** (Figure 5). In transition state **TS-IIIb-α**, the Pd–Ar bond has elongated to 2.060 Å, whilst the Pd–C_α distance is now 2.314 Å. The Pd···O interaction is lost in the TS and the C_α–C_{Ar} bond that forms is long (2.006 Å). From isomer **IIIa**, the reductive elimination is exoergic, with a Gibbs free reaction energy $\Delta G = -24.9$ kcal mol^{-1} in favor of α-arylated product **3a**.

The pathway leading to β-arylated product **4a** involves several steps. The agostic enolate complex **IIIa** leads to an olefin hydride intermediate (**IVa**) through a β–H-elimination TS (**TS-IIIa-IVa**); this intermediate is 10.3 kcal mol^{-1} higher in energy than complex **IIIa** (Figure 6) and is barely more stable than the preceding transition state **TS-IIIa-IVa**, which is 11.0 kcal mol^{-1} higher in energy than complex **IIIa**. The TS for β–H elimination is late, as confirmed by the geometrical parameters (C_β···H 1.946 Å and H···Pd 1.586 Å), and the C_α–C_β bond has shortened from 1.503 Å in complex **IIIa** to 1.409 Å in **TS-IIIa-IVa**. The geometrical parameters for intermediate **IVa** are only slightly different from those for **TS-IIIa-IVa** (C_β···H 1.997 Å, H–Pd 1.585 Å, C_α–C_β 1.406 Å). From intermediate **IVa**, olefin rotation leads to intermediate **IVb** through transition state **TS-IVa-IVb** (Figure 6). The activation barrier for the rotation is 7.5 kcal mol^{-1} and intermediate **IVb** is 6.8 kcal mol^{-1} less stable than intermediate **IVa**. In transition state **TS-IVa-IVb**, the olefin is roughly perpendicular to the Pd–Ar axis (Ar-Pd-C_β-C_α 74°). Once the olefin has experienced a 180° rotation, insertion into the Pd–H bond through **TS-IVb-V** affords homoenolate intermediate **V** in which the C_β atom is now attached to the Pd center. This insertion is easy ($\Delta G^{\#} = 2.7$ kcal mol^{-1}) and exoergic ($\Delta G = -13.1$ kcal mol^{-1}). Homoenolate **V** is only 4.0 kcal mol^{-1} less stable than enolate **IIIa** despite the fact that no stabilizing agostic interaction is present in compound **V** (Figure 6). One important feature of homoenolate **V** is the significantly stronger interactions between the biaryl group of DavePhos and the Pd center, as illustrated by the much-shortened Pd···C_{ipso} distance of 2.672 Å (C_{ipso} = *ipso*-carbon atom of the phenyl ring of DavePhos that bears an NMe_2 substituent). The Pd–C_{ipso} distances are about 3.6 Å for all of the extrema along the α-arylation pathway, and the same value is obtained for the extrema preceding compound **V** in the β-arylation pathway. Only transition state **TS-IVb-V** starts to show some increased interaction,

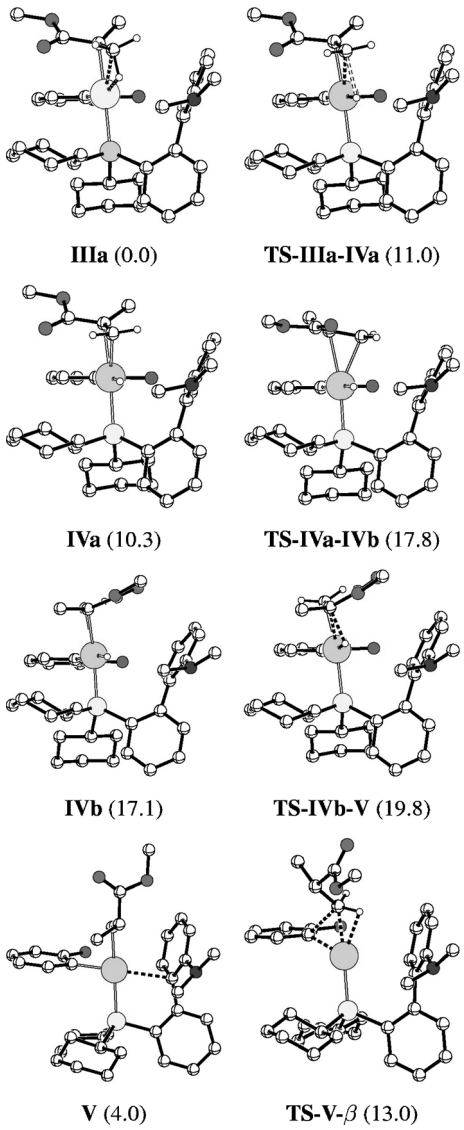

Figure 6. Optimized geometry and Gibbs free energy (kcal mol^{-1}, relative to **IIIa**) of the various intermediates and TSs along the β-arylation pathway.

with a Pd–C_{ipso} distance of 3.448 Å. Whereas the C–C coupling step from compound **IIIb** to give α-arylated product **3a** has an activation barrier of $\Delta G^{\#} = 21.4$ kcal mol^{-1} (Figure 5), the TS for C–C coupling that leads to β-arylated product **4a** (**TS-V-β**) is only 9.0 kcal mol^{-1} higher in energy than compound **V** (Figure 6). This lower activation barrier for C–C coupling can be explained by two factors: 1) the Pd···C_{ipso} distance in transition state **TS-V-β** (3.178 Å) suggests a stabilization of the developing Pd^0 character by the biaryl group of DavePhos;[17,30] 2) there is also an α-agostic interaction (C_β–H 1.116 Å, H···Pd 2.102 Å) that contributes to stabilize transition state **TS-V-β** (Figure 6). The reductive-elimination step, **V**→**Ia**+**4a**, is exoergic, with a Gibbs free energy of −33.7 kcal mol^{-1}. With respect to complex **IIIa**, β-arylated product **4a** lies at −29.7 kcal mol^{-1} and is thus the thermodynamic product of the reaction.

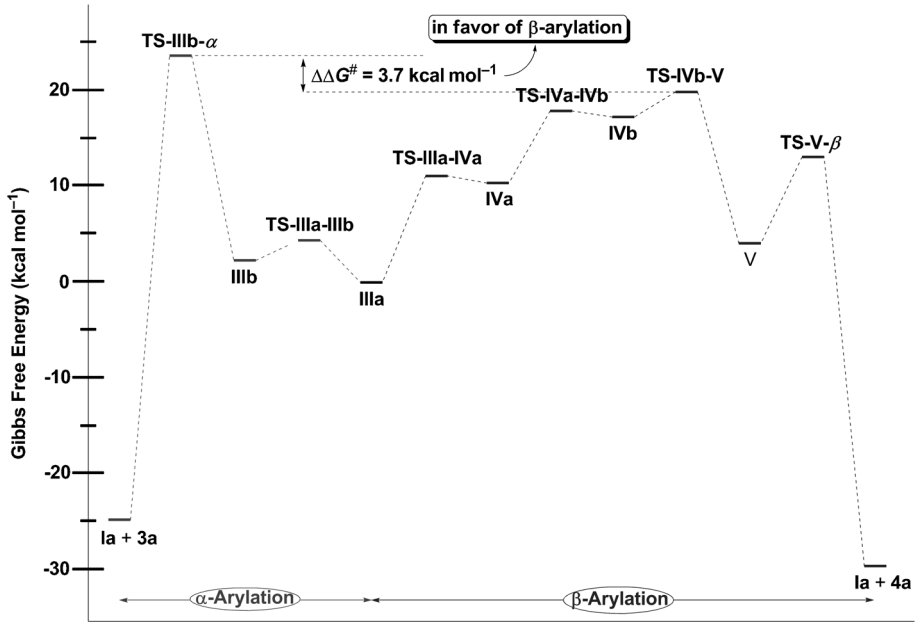

Figure 7. Comparison of the energy profiles for the α- and β-arylation pathways from enolate complex **IIIa** with DavePhos as the ligand.

A comparison of the α- and β-arylation pathways is shown in Figure 7. In addition to the thermodynamic preference for compound **4a** over compound **3a**, there is a clear kinetic preference for the β-arylation pathway ($\Delta\Delta G^{\#}=$ 3.7 kcal mol^{-1}). These calculated profiles are in perfect agreement with the experimental observations, where only compound **4a** is observed in the reaction between compounds **1a** and **2a**, catalyzed by [Pd(DavePhos)]. In the β-arylation pathway, the transition states **TS-IIIa-IVa** and **TS-IVa-IVb** lie at almost the same energies as their corresponding products (**IVa** and **IVb**, respectively). Thus, the β–H-elimination, olefin-rotation, and olefin-insertion steps actually behave as a single step that corresponds to the isomerization of Pd enolate **IIIa** into homoenolate **V**. This isomerization is the rate-limiting step of the β-arylation pathway, with an activation barrier of $\Delta G^{\#}=19.8$ kcal mol^{-1} (calculated as the energy difference between compound **IIIa** and the transition state **TS-IVb-V**). This analysis is in agreement with the intra- and intermolecular kinetic isotope effects observed experimentally (Scheme 4c,d). The 19.8 kcal mol^{-1} activation barrier is also in agreement with the reaction occurring at room temperature.

To study the influence of the biaryl group in DavePhos on the selectivity, the pathways for the α- and β-arylation reactions were computed for [Pd(PCy_3)] as the catalyst. The enolate complex **IIIa-Cy** presents the same overall geometry as that obtained for compound **IIIa**. There is a clear β–CH agostic interaction (C_β–H 1.166 Å, H···Pd 1.896 Å), and the bonds to Pd are similar to those obtained in compound **IIIa** (Pd–C_α 2.088 Å, Pd–Ar 2.010 Å). The only significant difference is in a shorter Pd–P bond in compound **IIIa-Cy** (Pd–P 2.405 Å for compound **IIIa** versus Pd–P 2.376 Å for compound **IIIa-Cy**). The shorter Pd–P bond in compound **IIIa-Cy** could be ascribed to the smaller steric impact of PCy_3 compared to DavePhos. This observation is further demonstrated by the relative energy of isomer **IIIb-Cy**, which is 1.1 kcal mol^{-1} lower in energy than isomer **IIIa-Cy**. The Pd···O distance is shorter in isomer **IIIb-Cy** (2.246 Å) than in compound **IIIb** (2.281 Å). The α-arylation pathway is barely affected, as transition state **TS-IIIb-α-Cy** is 23.8 kcal mol^{-1} higher in energy than **IIIa-Cy**. The thermodynamic driving force is not as strong as when DavePhos was used as the ligand; the Gibbs free reaction energy to form [Pd(PCy_3)] and **3a** is $\Delta G=-13.5$ kcal mol^{-1}. The more-negative value ($\Delta\Delta G\approx 10$ kcal mol^{-1}) when DavePhos is used as the ligand ($\Delta G=-24.9$ kcal mol^{-1}) is due to an extra stabilization of the [Pd(DavePhos)] complex through coordination of the aromatic ring that is not bonded to the phosphorous atom.[30] The β-arylation pathway with [Pd(PCy_3)] shows the decreased steric impact of the PCy_3 ligand compared to DavePhos; Figure 8 shows a comparison of the pathways with each phosphine. The β–H-elimination and olefin-rotation steps are slightly easier with PCy_3 as the ligand. The most-significant difference occurs for the rotated olefin intermediates **IVb** and **IVb-Cy**: In intermediate **IVb**, the COOMe ester group is proximal to the biphenyl group of DavePhos and, consequently, the intermediate is 17.1 kcal mol^{-1} higher in energy than compound **IIIa**. Such steric repulsion is not so stringent in intermediate **IVb-Cy** where the Cy group is smaller and the energy of intermediate **IVb-Cy** relative to **IIIa-Cy** is 12.5 kcal mol^{-1}. This difference is shown in the TSs for insertion into the Pd–H bond, where **TS-IVb-V** is 19.8 kcal mol^{-1} higher in energy than compound **IIIa** whereas **TS-IVb-V-Cy** is only 13.8 kcal mol^{-1} higher in energy than compound **IIIa-Cy**. In the case of DavePhos, the insertion TS is the highest point along the β-arylation pathway, whereas with PCy_3 the TS for the olefin rotation is the highest point. However, in the latter case there is no stabilizing influence of the phosphine ligand, neither in the homoenolate intermediate **V-Cy** nor in the TS for C–C reductive elimination (**TS-V-β-Cy**). Homoenolate **V-Cy** is 5.9 kcal mol^{-1} less stable than enolate **IIIa-Cy**, whereas enolate **V** is only 4 kcal mol^{-1} less stable than compound **IIIa**. This difference in stability is enhanced in the TS of the C–C-coupling step, where effective interaction with DavePhos lays **TS-V-β** at 13.0 kcal mol^{-1} higher in energy than compound **IIIa**, whilst **TS-V-β-Cy** is 16.1 kcal mol^{-1} higher in energy than **IIIa-Cy**. With PCy_3, the TS in the reductive-elimination step

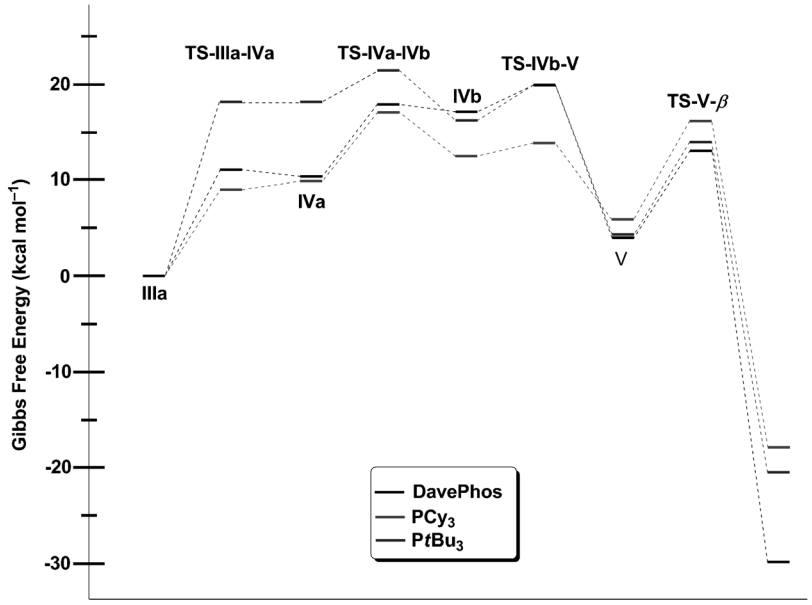

Figure 8. Comparison of the energy profiles for the β-arylation pathway from enolate complex **IIIa** with three different phosphine ligands.

is only 0.9 kcal mol^{-1} below the TS of the olefin rotation and the nature of the rate-determining step is different compared to DavePhos. However, the β-arylation pathway is also clearly preferred both kinetically and thermodynamically over the α-arylation pathway ($\Delta\Delta G^{\#}=6.8$ kcal mol^{-1} and $\Delta\Delta G=4.3$ kcal mol^{-1}, respectively), which is in agreement with the experimental observation that only compound **4a** is produced in the reaction between **1a** and **2a**, catalyzed by [Pd(PCy$_3$)].

Thus, the β-arylation pathway seems to be strongly affected by the steric bulk of the phosphine ligand, whereas the α-arylation pathway seems to be less sensitive to the steric demands of the ligand. Therefore, if drastic modifications are made on the phosphine ligand, an inversion of the selectivity may be obtained. This is indeed what is observed experimentally in the reaction of compounds **1a** and **2a** catalyzed by P*t*Bu$_3$ (Figure 1), where α-arylated product **3a** is obtained preferentially over β-arylated product **4a** (85:15 ratio). The α- and β-arylation pathways were computed with the P*t*Bu$_3$ ligand and the first significant change observed is the easier overall α-arylation reaction pathway, with transition state **TS-IIIb-α-*t*Bu** lying at 21.2 kcal mol^{-1} higher in energy than compound **IIIa-*t*Bu**. This result could be explained by a larger steric impact of this phosphine ligand, which facilitates the reductive-elimination step.[1a,31] The easier reductive-elimination step with the bulkier P*t*Bu$_3$ ligand is also observed in the β-arylation pathway, where **TS-V-β-*t*Bu** lies at 13.9 kcal mol^{-1} higher in energy than compound **IIIa-*t*Bu** (Figure 8). However, the steric impact of P*t*Bu$_3$ is clearly evident on the TS for olefin rotation: transition state **TS-IVa-IVb-*t*Bu** is 21.4 kcal mol^{-1} higher in energy than compound **IIIa-*t*Bu**, that is 4 kcal mol^{-1} higher than with PCy$_3$.[32] This TS is the highest point along the β-arylation pathway and now the selectivity has been reversed with a $\Delta\Delta G^{\#}$ value of 0.2 kcal mol^{-1} in favor of the formation of α-arylated product **3a**. However, this value (0.2 kcal mol^{-1}) does not correspond to the 85:15 ratio observed experimentally, but the qualitative trend is very well reproduced by the calculations.

The reaction profiles with [Pd(DavePhos)] and [Pd(PCy$_3$)] (Figure 8) do not explain why the reaction with PCy$_3$ is not efficient at 50 °C and why heating to 110 °C is necessary. In palladium-catalyzed cross-coupling reactions, the efficiency of the catalysis is related to the ease with which the necessary reactive species are formed. For the C–X oxidative-addition step, a monoligated [Pd(L)] complex is preferred, hence bulky phosphines, like P*t*Bu$_3$, are efficient ligands for this step.[33] Once the oxidative addition has been performed, it is necessary to maintain a vacant site on the [Pd(Ar)(L)(X)] complex for substitution of X by the other partner, in this case the enolate, along an associative pathway.[34] This vacant site may be trapped by a coordinating solvent, a free phosphine, or by another molecule of [Pd(Ar)(L)(X)], thus forming a dimer as observed experimentally with DavePhos (Figure 3). This dimer has been optimized and the computed geometry of compound **IId** is in very good agreement with the experimental structure **IIb** (Figure 9). The computed N···Pd distance is longer than the experimentally determined value (3.34 Å versus 3.2 Å). Dissociation of the dimer, whilst maintaining the vacant site *trans* to the Ar group affords compound **IIe** that is 7.1 kcal mol^{-1} higher in energy than compound **IId**. The N···Pd distance is shortened to 3.07 Å in compound **IIe**. However, as already shown by Barder et al. for other biarylphosphines,[17] the DavePhos ligand is able to form a secondary interaction between the biaryl group and the metal. This interaction is indeed effective in compound

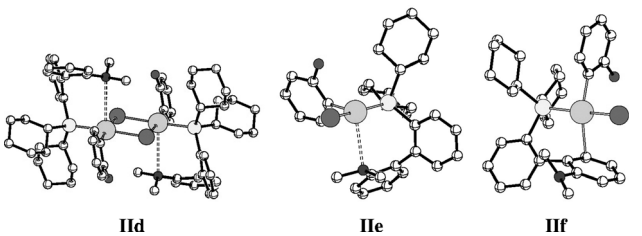

Figure 9. Optimized geometry for the dimer [{Pd(2-FC$_6$H$_4$)(μ-Br)(DavePhos)}$_2$] (**IId**) and the two isomers for the monomer [Pd(2-FC$_6$H$_4$)(Br)(DavePhos)] (**IIe** and **IIf**).

IIf (Figure 9), an isomer of compound **IIe**, where a close contact is evident between the unsubstituted *ortho* carbon and Pd atoms (Pd···C_{ortho} 2.572 Å). As a result, compound **IIf** is 12.3 kcal mol^{-1} more stable than compound **IIe** and the equilibrium **IId**⇔**IIf**+**IIf** is strongly exoergic ($\Delta G = -17.5$ kcal mol^{-1}). The biaryl···Pd interaction effectively shields the metal center from adventitious coordination that would reduce the catalytic activity. The exoergicity of the equilibrium for dimer dissociation is certainly overestimated as the entropy contributions in the condensed phase are lower than the values calculated in the gas phase. Nevertheless, the PCM value for the equilibrium ($\Delta E = 0.2$ kcal mol^{-1}) clearly indicates that the dimer easily dissociates. This observation is in agreement with the fact that dimer **IIb** is a competent catalyst for the β-arylation reaction of enolates.

Computational experiments were also performed for the dimer with PCy_3 as the phosphine ligand (**IId-Cy**), and the corresponding monomer **IIe-Cy** only exhibits limited protection of the vacant site by one C–H bond of a cyclohexyl group (H···Pd 2.475 Å). The equilibrium is slightly in favor of the monomer ($\Delta G = -1.3$ kcal mol^{-1}), but the origin of this stability is essentially entropic as the corresponding PCM ΔE value is 18.3 kcal mol^{-1}. With respect to dissociation, dimer **IId-Cy** is 18.1 kcal mol^{-1} more stable than the dimer with DavePhos (**IId**) and therefore, the equilibrium **IId-Cy**⇔**IIe-Cy**+**IIe-Cy** is likely to have a stronger impact on the overall reactivity than the corresponding equilibrium for the DavePhos system. This result might explain why a higher temperature is required with PCy_3 to observe significant conversion. The PCy_3 ligand does not afford enough protection of the vacant site on Pd during some crucial steps and any molecule that is able to interact with the metal could deactivate the catalyst at room temperature. This result explains why [Pd(2-FC_6H_4)(Br)(PCy_3)$_2$] (**IIc**; Figure 3) is not a competent catalyst, as, even if [Pd(2-FC_6H_4)(Br)(PCy_3)] could be generated,[35] there will be a competition between the enolate and the free PCy_3 group for binding to the vacant site.

As illustrated in Figure 1, the biarylphosphine family of ligands is particularly well-adapted to the β-arylation of ester enolates, as it provides the best compromise between efficient steric protection and easy generation of a reactive vacant site through isomerization of the biaryl group. However, the selectivity between the α- and β-arylation pathways strongly depends on the nature of the aryl electrophile (Table 1). To shed more light on these results, the competition between the α- and β-arylation pathways was studied computationally for the reaction of ester **2a** with selected aryl bromides. The only difference between the computed and experimental systems was in the nature of the ester group (Me versus *t*Bu), but the latter was already shown experimentally to have only a minor effect on the reaction. The α- and β-arylation pathways were studied in detail for *m*- (**1b**) and *p*-fluorobromobenzene (**1c**) and the results were similar to those obtained with *o*-fluorobromobenzene (**1a**), with the highest point on the β-arylation pathway also being the TS for olefin insertion into the Pd–H bond. Consequently, for the other aryl bromides, only the insertion TS was computed together with the Pd–enolate complex and the TS for the reductive-elimination step along the α-arylation pathway. Table 2 shows the activation barriers for the α- and β-arylation pathways, and displays the computed and experimental $\Delta\Delta G^{\#} = \Delta G^{\#}_{\beta} - \Delta G^{\#}_{\alpha}$ values.

Table 2. Computed activation barriers (kcal mol^{-1}) along the α- ($\Delta G^{\#}_{\alpha}$) and β-arylation ($\Delta G^{\#}_{\beta}$) pathways, and comparison of calculated and experimental kinetic selectivities for the α- and β-arylation reactions ($\Delta\Delta G^{\#}$).

Entry	Aryl bromide	$\Delta G^{\#}_{\alpha}$ [a]	$\Delta G^{\#}_{\beta}$ [a]	$\Delta\Delta G^{\#}_{calcd}$ [b]	$\Delta\Delta G^{\#}_{exp}$ [b]
1	**1a**	23.5	19.8	−3.7	< −2.3
2	**1b**	20.4	20.7	0.3	−0.07
3	**1c**	20.2	20.3	0.1	−0.07
4	**1d**	19.5	20.4	0.9	0.9
5	**1e**	20.0	20.6	0.6	0.6
6	**1h**	19.9	20.6	0.7	1.0
7	**1i**	19.6	20.3	0.7	0.8
8	**1l**	21.5	20.7	−0.8	−0.2
9	**1m**	21.1	20.7	−0.4	0.3
10	**1o**	21.1	19.3	−1.8	−1.8

[a] Calculated values. [b] $\Delta\Delta G^{\#} = \Delta G^{\#}_{\beta} - \Delta G^{\#}_{\alpha}$. A negative value for $\Delta\Delta G^{\#}$ indicates that the β-arylated product is kinetically preferred.

The trend observed experimentally for the competition between α- and β-arylation is particularly well reproduced by the calculations ($|\Delta\Delta G^{\#}_{calcd} - \Delta\Delta G^{\#}_{exp}| \leq 0.7$ kcal mol^{-1}). The results in Table 2 indicate that the α-arylation pathway is more sensitive to variation in the nature of the aryl ring. This result is not surprising, as α-arylation involves cleavage of the Pd–Ar bond as the rate-determining step where any factor that renders the Pd–Ar bond stronger would disfavor the reaction.[31] This influence is indeed what is observed when electron-withdrawing groups are placed at the *ortho* position (Table 1, entries 1, 7, 10), where it has been shown that the resulting Pd–C_{Ar} bond is significantly stronger than when the substituents are placed at other positions.[36] The activation barrier for α-arylation in the case of compound **1a** (Table 2, entry 1) stands in marked contrast with the other values (Table 2, entries 2–10). In contrast, apart from the case of compound **1o** (Table 2, entry 10), the activation barriers for β-arylation span a much-narrower range of values. This result is not surprising as the electronic influence of the substituent on the cleavage of the Pd–Ar bond occurs after the rate-determining step. As already discussed, the C–C reductive-coupling step along the β-arylation pathway is less affected by the electronic properties of the aryl bromide because it benefits from the stabilizing influence of an α-CH agostic interaction and from the interaction between the biaryl group of DavePhos and Pd. The results in Table 2 show that, as soon as no electron-withdrawing group is present in the *ortho* position of the aryl bromide, the α- and β-arylation pathways are associated with activation barriers of similar magnitude. However, introducing electron-withdrawing groups onto the *meta* and/or *para* position(s) of the aryl ring seems to destabilize the α-arylation route suffi-

ciently to increase the proportion of β-arylated product to a significant extent (Table 2, entries 8–10).

Biaryldialkylphosphines seem to constitute the most-well-adapted family of ligands for achieving significant selectivity in favor of β-arylation at mild temperatures with aryl bromide **1a** (Figure 1).[6] For instance, PCy_3 requires a higher temperature and $PtBu_3$ gives mostly α-arylation products. However, the substitution pattern of the biaryl group has a critical influence on α/β-arylation selectivity in the case of aryl bromide **1b** (Figure 2), with DavePhos being currently the optimal ligand. Further studies are needed to better understand this behavior and to design more selective ligands for a broader range of β-arylation reactions. In addition, a detailed analysis of the effect of the enolate structure on the selectivity of the arylation reaction will be reported in due course.

Conclusion

The palladium-catalyzed β-arylation of ester enolates with aryl bromides was studied in detail both experimentally and computationally. First, the effect of the ligand on the selectivity of the α/β-arylation reactions of *ortho*- and *meta*-fluorobromobenzene (**1a** and **1b**, respectively) was described. Whereas β-arylation was predominantly observed with *o*-fluorobromobenzene (**1a**) for a range of biarylphosphine ligands, α-arylation was primarily observed with *m*-fluorobromobenzene (**1b**) for all ligands except with DavePhos ($\mathbf{L^2}$), which gave an approximate 1:1 mixture of α-/β-arylated products. Next, the effect of the substitution pattern of the aryl-bromide reactant was studied with DavePhos as the ligand. We showed that electronic factors played a major role in the α/β-arylation selectivity, with electron-withdrawing substituents favoring β-arylation. In addition, electron-withdrawing substituents had the most influence when they were at the *ortho* position, and steric factors contributed only marginally. The reaction mechanism was studied experimentally with DavePhos as the ligand. Kinetic and deuterium-labeling experiments suggested that the rate-limiting step of β-arylation was the palladium-enolate-to-homoenolate isomerization (**III**→**V**), which occurs by a β–H-elimination, olefin-rotation, and olefin-insertion sequence. A dimeric oxidative-addition complex (**IIb**) was isolated and structurally characterized. This complex was shown to be not only catalytically competent, but also more active than the $[Pd_2(dba)_3]$/DavePhos in situ mixture. A common mechanism for α- and β-arylation was described by DFT calculations performed at the B3PW91 level. These calculations agreed with experimental observations. With DavePhos as the ligand, the pathway leading to β-arylation was kinetically favored over the pathway leading to α-arylation, with the palladium-enolate-to-homoenolate isomerization being the rate-limiting step of the β-arylation pathway and the TS for olefin insertion (**TS-IVb-V**) its highest point. The nature of the rate-limiting step changed with PCy_3 and $PtBu_3$ ligands, and with the latter, α-arylation became kinetically favored. The trend in selectivity observed experimentally with differently substituted aryl bromides agreed well with that observed from the calculations. The presence of electron-withdrawing groups on these bromides mainly affected the α-arylation pathway by disfavoring C–C reductive elimination. Finally, we concluded that the higher activity of the biaryldialkylphosphine ligands, compared to their corresponding trialkylphosphines, could be attributed to stabilizing interactions between the biaryl backbone of the ligands and the metal center, thereby preventing deactivation of the β-arylation pathway. However, the exact role of the biaryl substituents, culminating with the unique trend in selectivity observed with DavePhos, is still elusive and will constitute the matter of future studies.

Acknowledgements

This work was supported by the Université Claude Bernard Lyon 1, ANR (programme blanc "AlCaCHA") and the Institut Universitaire de France. We also thank Dr. E. Jeanneau (UCBL) for crystallographic data collection, structure solution, and refinement.

[1] a) D. A. Culkin, J. F. Hartwig, *Acc. Chem. Res.* **2003**, *36*, 234–245; b) C. C. C. Johansson, T. J. Colacot, *Angew. Chem.* **2010**, *122*, 686–718; *Angew. Chem. Int. Ed.* **2010**, *49*, 676–707; c) F. Bellina, R. Rossi, *Chem. Rev.* **2010**, *110*, 1082–1146.
[2] a) M. Kawatsura, J. F. Hartwig, *J. Am. Chem. Soc.* **1999**, *121*, 1473–1478; b) D. A. Culkin, J. F. Hartwig, *J. Am. Chem. Soc.* **2001**, *123*, 5816–5817; c) S. Lee, J. F. Hartwig, *J. Org. Chem.* **2001**, *66*, 3402–3415; d) D. A. Culkin, J. F. Hartwig, *J. Am. Chem. Soc.* **2002**, *124*, 9330–9331; e) J. P. Wolkowski, J. F. Hartwig, *Angew. Chem.* **2002**, *114*, 4465–4467; *Angew. Chem. Int. Ed.* **2002**, *41*, 4289–4291.
[3] a) R. Jazzar, J. Hitce, A. Renaudat, J. Sofack-Kreutzer, O. Baudoin, *Chem. Eur. J.* **2010**, *16*, 2654–2672; b) O. Baudoin, *Chem. Soc. Rev.* **2011**, *40*, 4902–4911.
[4] a) D. Shabashov, O. Daugulis, *Org. Lett.* **2005**, *7*, 3657–3659; b) V. G. Zaitsev, D. Shabashov, O. Daugulis, *J. Am. Chem. Soc.* **2005**, *127*, 13154–13155; c) B. V. S. Reddy, L. R. Reddy, E. J. Corey, *Org. Lett.* **2006**, *8*, 3391–3394; d) R. Giri, N. Maugel, J.-J. Li, D.-H. Wang, S. P. Breazzano, L. B. Saunders, J.-Q. Yu, *J. Am. Chem. Soc.* **2007**, *129*, 3510–3511; e) M. Wasa, K. M. Engle, J.-Q. Yu, *J. Am. Chem. Soc.* **2009**, *131*, 9886–9887; f) M. Wasa, J.-Q. Yu, *Tetrahedron* **2010**, *66*, 4811–4815; g) D. Shabashov, O. Daugulis, *J. Am. Chem. Soc.* **2010**, *132*, 3965–3972; h) Y. Feng, G. Chen, *Angew. Chem.* **2010**, *122*, 9943; *Angew. Chem. Int. Ed.* **2010**, *49*, 958–961; i) Y. Feng, Y. Wang, B. Landgraf, S. Liu, G. Chen, *Org. Lett.* **2010**, *12*, 3414–3417.
[5] M. Jørgensen, S. Lee, X. Liu, J. P. Wolkowski, J. F. Hartwig, *J. Am. Chem. Soc.* **2002**, *124*, 12557–12565.
[6] A. Renaudat, L. Jean-Gérard, R. Jazzar, C. E. Kefalidis, E. Clot, O. Baudoin, *Angew. Chem.* **2010**, *122*, 7419–7423; *Angew. Chem. Int. Ed.* **2010**, *49*, 7261–7265.
[7] For recent reviews: a) D. S. Surry, S. L. Buchwald, *Angew. Chem.* **2008**, *120*, 6438–6461; *Angew. Chem. Int. Ed.* **2008**, *47*, 6338–6361; b) D. S. Surry, S. L. Buchwald, *Chem. Sci.* **2011**, *2*, 27–50.
[8] H. Tomori, J. M. Fox, S. L. Buchwald, *J. Org. Chem.* **2000**, *65*, 5334–5341.
[9] C. A. Parrish, S. L. Buchwald, *J. Org. Chem.* **2001**, *66*, 3820–3827.
[10] C. Han, S. L. Buchwald, *J. Am. Chem. Soc.* **2009**, *131*, 7532–7533.
[11] Chieffi, K. Kamikawa, J. Åhman, J. M. Fox, S. L. Buchwald, *Org. Lett.* **2001**, *3*, 1897–1900.
[12] J. Yin, M. P. Rainka, X.-X. Zhang, S. L. Buchwald, *J. Am. Chem. Soc.* **2002**, *124*, 1162–1163.

[13] For comparison, the Tolman cone angles (θ) of related PR_3 phosphines are as follows:[14] $PtBu_3$ 182°, PCy_3 170°, $PiPr_3$ 160°, PPh_3 143°.
[14] a) C. A. Tolman, *Chem. Rev.* **1977**, *77*, 313–348; b) T. L. Brown, K. J. Lee, *Coord. Chem. Rev.* **1993**, *128*, 89–116.
[15] Reactions of aryl bromides with an *ortho* substituent were slower and thus they were all conducted at 50 °C instead of 30 °C.
[16] U. Christmann, R. Vilar, *Angew. Chem.* **2005**, *117*, 370–378; *Angew. Chem. Int. Ed.* **2005**, *44*, 366–374.
[17] a) T. E. Barder, S. D. Walker, J. R. Martinelli, S. L. Buchwald, *J. Am. Chem. Soc.* **2005**, *127*, 4685–4696; b) T. E. Barder, M. R. Biscoe, S. L. Buchwald, *Organometallics* **2007**, *26*, 2183–2192.
[18] Y. Pan, G. B. Young, *J. Organomet. Chem.* **1999**, *577*, 257–264.
[19] For details, see the Supporting Information.
[20] With SPhos **L[4]**, see: a) M. R. Biscoe, T. E. Barder, S. L. Buchwald, *Angew. Chem.* **2007**, *119*, 7370–7373; *Angew. Chem. Int. Ed.* **2007**, *46*, 7232–7235; with BrettPhos **L[9]**: b) B. P. Fors, D. A. Watson, M. R. Biscoe, S. L. Buchwald, *J. Am. Chem. Soc.* **2008**, *130*, 13552–13554; with KenPhos **L[10]**: c) X. Shen, G. O. Jones, D. A. Watson, B. Bhayana, S. L. Buchwald, *J. Am. Chem. Soc.* **2010**, *132*, 11278–11287.
[21] This distance corresponds to the sum of the van der Waals radii of N and Pd atoms (3.18 Å); thus, this interaction should be essentially electrostatic. For recent examples of square-pyramidal Pd complexes with an apical nitrogen ligand, see: a) M. Kujime, S. Hikichi, M. Akita, *Chem. Lett.* **2003**, *32*, 486–487; b) X. Zhang, Q. Xia, W. Chen, *Dalton Trans.* **2009**, 7045–7054 and the references therein.
[22] CCDC-845801 (**IIb**) and CCDC-845802 (**IIc**) contain the supplementary crystallographic data for this paper. These data can be obtained free of charge from The Cambridge Crystallographic Data Centre via www.ccdc.cam.ac.uk/data_request/cif.
[23] a) C. Amatore, A. Jutand, F. Khalil, M. A. M'Barki, L. Mottier, *Organometallics* **1993**, *12*, 3168–3178; for a review: b) I. J. S. Fairlamb, *Org. Biomol. Chem.* **2008**, *6*, 3645–3656.
[24] For a mechanistic study of β–H elimination from Pt–enolate complexes, see: E. J. Alexanian, J. F. Hartwig, *J. Am. Chem. Soc.* **2008**, *130*, 15627–15635.
[25] Benzyl esters were chosen because they were easier to prepare, and aryl bromide **1p** was chosen instead of compound **1a** because the corresponding products were easier to analyze by NMR spectroscopy.
[26] M. Gómez-Gallego, M. A. Sierra, *Chem. Rev.* **2011**, *111*, 4857–4963.
[27] For related isomerizations, see: a) J. P. Wolfe, *Eur. J. Org. Chem.* **2007**, 571–582; b) S. Seel, T. Thaler, K. Takatsu, C. Zhang, H. Zipse, B. F. Straub, P. Mayer, P. Knochel, *J. Am. Chem. Soc.* **2011**, *133*, 4774–4777.
[28] A similar explanation was put forward for Pd- and Ni-catalyzed ethylene polymerization reactions: a) L. K. Johnson, C. M. Killian, M. Brookhart, *J. Am. Chem. Soc.* **1995**, *117*, 6414–6415; b) L. K. Johnson, S. Mecking, M. Brookhart, *J. Am. Chem. Soc.* **1996**, *118*, 267–268; c) L. Deng, P. Margl, T. Ziegler, *J. Am. Chem. Soc.* **1997**, *119*, 1094–1100; d) L. H. Shultz, M. Brookhart, *Organometallics* **2001**, *20*, 3975–3982.
[29] For related studies in the context of $C(sp^3)$–H bond functionalization, see: a) M. Chaumontet, R. Piccardi, N. Audic, J. Hitce, J.-L. Peglion, E. Clot, O. Baudoin, *J. Am. Chem. Soc.* **2008**, *130*, 15157–15166; b) S. Rousseaux, M. Davi, J. Sofack-Kreutzer, C. Pierre, C. E. Kefalidis, E. Clot, K. Fagnou, O. Baudoin, *J. Am. Chem. Soc.* **2010**, *132*, 10706–10716.
[30] T. E. Barder, S. L. Buchwald, *J. Am. Chem. Soc.* **2007**, *129*, 12003–12010.
[31] J. F. Hartwig, *Inorg. Chem.* **2007**, *46*, 1936–1947.
[32] The transition state **TS-IIIa-IVa-*t*Bu** could not be located and it was assumed to have the same energy as the intermediate **IVa-*t*Bu**.
[33] G. C. Fu, *Acc. Chem. Res.* **2008**, *41*, 1555–1564.
[34] C. E. Kefalidis, O. Baudoin, E. Clot, *Dalton Trans.* **2010**, *39*, 10528–10535.
[35] $[Pd(2\text{-}FC_6H_4)(Br)(PCy_3)_2]$ and $[Pd(2\text{-}FC_6H_4)(Br)(PCy_3)]$ were optimized and the phosphine dissociation was associated to a PCM value of $\Delta E = 15.4$ kcal mol^{-1}.
[36] a) E. Clot, C. Mégret, O. Eisenstein, R. N. Perutz, *J. Am. Chem. Soc.* **2009**, *131*, 7817–7827; b) M. E. Evans, C. L. Burke, S. Yaibuathes, E. Clot, O. Eisenstein, W. D. Jones, *J. Am. Chem. Soc.* **2009**, *131*, 13464–13473; c) T. Tanabe, W. W. Brennessel, E. Clot, O. Eisenstein, W. D. Jones, *Dalton Trans.* **2010**, *39*, 10495–10509; d) J. Guihaumé, E. Clot, O. Eisenstein, R. N. Perutz, *Dalton Trans.* **2010**, *39*, 10510–10519.

Received: October 6, 2011
Published online: January 13, 2012

